

Recent advances and future challenges for massive MIMO channel measurements and models

Cheng-Xiang WANG^{1,2*}, Shangbin WU¹, Lu BAI², Xiaohu YOU³,
Jing WANG⁴ & Chih-Lin F⁵

¹*School of Engineering and Physical Sciences, Heriot-Watt University, Edinburgh EH14 4AS, U.K.;*

²*Shandong Provincial Key Laboratory of Wireless Communication Technologies, Shandong University, Jinan 250100, China;*

³*National Mobile Communications Laboratory, Southeast University, Nanjing 211189, China;*

⁴*Department of Electronic Engineering, Tsinghua University, Beijing 100084, China;*

⁵*China Mobile Research Institute, Beijing 100053, China*

Received August 30, 2015; accepted September 29, 2015; published online January 5, 2016

Abstract The emerging fifth generation (5G) wireless communication system raises new requirements on spectral efficiency and energy efficiency. A massive multiple-input multiple-output (MIMO) system, equipped with tens or even hundreds of antennas, is capable of providing significant improvements to spectral efficiency, energy efficiency, and robustness of the system. For the design, performance evaluation, and optimization of massive MIMO wireless communication systems, realistic channel models are indispensable. This article provides an overview of the latest developments in massive MIMO channel measurements and models. Also, we compare channel characteristics of four latest massive MIMO channel models, such as receiver spatial correlation functions and channel capacities. In addition, future challenges and research directions for massive MIMO channel measurements and modeling are identified.

Keywords 5G, massive MIMO channel measurements, massive MIMO channel models, non-stationary statistical properties, channel capacity

Citation Wang C X, Wu S B, Bai L, et al. Recent advances and future challenges for massive MIMO channel measurements and models. *Sci China Inf Sci*, 2016, 59(2): 021301, doi: 10.1007/s11432-015-5517-1

1 Introduction

The increasing demand for high-speed reliable communications with significantly improved user experience drives the development of the fifth generation (5G) wireless communication networks. It has been widely accepted that the capacity of the 5G wireless communication system should achieve 1000 times of that of the fourth generation (4G) long-term evolution advanced (LTE-A) wireless communication system [1–10]. Also, the spectral efficiency of the 5G system is required to reach 3–5 times with respect to the current 4G LTE-A system. As a result, the spectral efficiency of 5G is equivalent to 50 Gbps peak data rate for low mobility users. The METIS project even expects the 5G system to have 10 to 100 times higher data rates for typical users [7].

* Corresponding author (email: cheng-xiang.wang@hw.ac.uk)

In addition to the conventional spectral efficiency requirements, other key performance indicators (KPIs) have been considered in the design of 5G wireless communication networks in comparison to 4G networks. To enable longer battery lifetime for devices, energy efficiency that measures the transmitted bit per Joule needs to be improved by 10 times [1]. The traffic volume density (TVD) describes data throughput per unit area. It was reported in [7,8] that the goal for 5G is to increase the TVD by a factor of 1000. The ability to process a massive number of devices will be compulsory as there will be billions of connected devices in the 5G wireless communication network by 2020 [3]. The 5 times reduced end-to-end (E2E) latency will play an important role in improving user experience [3]. It is also anticipated that coexistence of multiple radio access technologies (multi-RATs) is inevitable in 5G wireless communication networks [1–9]. Moreover, more scenarios such as high-speed train (HST) communications, machine-to-machine (M2M) communications, and low power massive machine communication will be supported in 5G. In order to satisfy the above-mentioned requirements, advanced technologies such as millimeter wave (mmWave) techniques, denser small cells, soft defined air interface (SDAI), and high-efficiency multiple antenna techniques will be key components of 5G wireless communication networks [3,4,6,10].

The employment of more spectrum is three-fold. First, it was suggested in [4] that underutilized allocated spectrum should be better explored. Second, spectrum flexibility can be improved by authorized shared access (ASA), which is optimal for small cells, and using unpaired spectrum allocations [3]. Third, higher frequency bands such as mmWave bands are able to provide large bandwidths for 5G wireless communication systems [1,2,10].

Denser smaller cells bring the network closer to every user. Therefore, the data rate of the network can be boosted. The application of denser small cells is straightforward and effective, which has attracted the attention of many wireless vendors [1–5].

To support various services and applications, adaptations of resources of air interface such as frame structure, bandwidth, waveform will be achieved in SDAI [6]. As a result, customized air interface is highly scalable and configurable. It is expected that SDAI would be a favorable solution for 5G air interface [6].

Recently, massive multiple-input multiple-output (MIMO) technology has appealed to many researchers due to its promising capability of greatly improving spectral efficiency, energy efficiency, and robustness of the system. In a massive MIMO system, both the transmitter and receiver are equipped with a large number of antenna elements (typically tens or even hundreds). It should be noticed that the transmit antennas can be co-located or distributed in different applications. Also, the enormous number of receive antennas can be possessed by one device or distributed to many devices. A massive MIMO system can not only enjoy the benefits of conventional MIMO systems, but also significantly enhance both spectral efficiency and energy efficiency [11–13]. Furthermore, as reported in [12], a massive MIMO system can be built with low-cost components because the linear requirement of the antenna amplifiers is low when each antenna is assigned with less power. By properly using multi-user MIMO (MU-MIMO) in massive MIMO systems, the multiple access control (MAC) layer design can be simplified by avoiding complicated scheduling algorithms. Consequently, these main advantages enable the massive MIMO technique to be a promising candidate for the 5G wireless communication networks [10,14–16].

Although massive MIMO systems can offer many advantages, there are several major challenges that have to be addressed before their practical deployment. First, it is essential for the transmitter to acquire the channel state information (CSI) to fully enjoy the capacity gain offered by massive MIMO systems, especially for multi-user scenarios. However, as the number of antennas increases, the overhead of acquiring CSI grows accordingly. This issue can be partially solved in a time division duplex (TDD) system which reduces the overhead of CSI by utilizing the reciprocity of the channel [13]. On the other hand, applications of massive MIMO to frequency division duplex (FDD) systems is still an open problem under discussion. Second, in [13] it was pointed out that the complexity of precoding and detection will rise with the number of antennas. When the number of transmit antennas is much larger than the number of receive antennas, simple linear precoders and detectors are sufficient to offer near-optimal performance. However, when the number of transmit antennas is comparable to or less than the number of receive antennas, the design of precoders and detectors with reasonable complexity becomes more

challenging. Third, how we can squeeze a large number of antennas into a limited area/volume while still maintaining low correlations remains an open problem. Finally, since the increase of antennas at the transceivers introduces new phenomenon such as nearfield effects and non-stationary effects [17], conventional MIMO channel models such as the WINNER II [18] and COST 2100 [19–21] channel models fail to capture these features and therefore, cannot be directly used as massive MIMO channel models.

There has been significant progress on channel measurements and models for massive MIMO recently. The main objective of this article is to give an overview of these recent advances as well as identifying future challenges and research directions. To sum up, the contributions of this paper can be listed as follows:

1. Recent advances in massive MIMO channel measurements and models are summarized.
2. Challenges and future research directions for channel measurements and models for massive MIMO are identified.

The remainder of this article is organized as follows. Recent advances, potential challenges, and future directions of massive MIMO channel measurements are discussed in Section 2. Section 3 investigates recent advances, potential challenges, and future directions of massive MIMO channel models. Finally, conclusions are drawn in Section 4.

2 Massive MIMO channel measurements

2.1 Recent advances in massive MIMO channel measurements

For studying realistic characteristics of massive MIMO channels, measurements on benefits and effects caused by the increasing number of antennas are crucial. There are many papers on recent advances in massive MIMO channel measurements. For comparison convenience, measurement settings and investigated channel characteristics in these papers are listed in Table 1.

2.1.1 Capacity

It was demonstrated via measurements in [17,22–32] that massive MIMO systems can significantly improve spectral efficiency. In [25], a scalable hardware architecture based on an FPGA platform was described and certain measurement results as well as implementation aspects were discussed. It was shown in [25] that the spectral efficiency grew nearly linearly with the number of antennas of massive MIMO, as suggested by theory.

In [23,24,27,28], it was shown that low-complexity linear processing algorithms were able to provide sufficiently good performance in terms of capacity due to high interchannel orthogonality of massive MIMO. At the same time, high-complexity processing algorithms (e.g., dirty-paper coding) were capable of providing relatively small gains but with much higher computational complexity. Additionally, it was stated in [30] that capacity gains of massive MIMO in a realistic measured channel can be achieved with simple linear precoding and even a reasonable number of antennas.

Average mutual couplings were studied in the measurement campaigns in [31,33]. Comparisons between massive MIMO channels and independent and identically distributed (i.i.d) channels were discussed in [24,29,30].

2.1.2 Spherical wavefront and non-stationarity

Measurements on massive MIMO channels in [17,36] demonstrated that the channel cannot be regarded as wide sense stationary (WSS) over the large antenna array. First, the farfield assumption, which is equivalent to plane wavefront approximation, is violated because the distances between the transmitter and receiver (scatterer) may not be beyond the Rayleigh distance. Second, certain clusters are not observable over the whole array. That is to say, each antenna element on the large array may have its own set of clusters. Third, power imbalance and Rician K-factor variation over the antenna array are seen as well. These three factors of massive MIMO channels indicate that the conventional modeling method of MIMO channels needs to be extended.

Table 1 Recent advances in massive MIMO channel measurements

Ref.	Scenario	Carrier frequency (GHz)	Array setting	Channel characteristics
[17]	Outdoor	2.6	Virtual ULA 128×1	spatial correlation, K-factor, APS, eigenvalue distribution channel gain, etc.
[22]	Indoor	5.6	Virtual 2-D antenna array $1 \times (12 \times 12)$	inverse condition number, RMS delay spread, etc.
[23]	Out-In In-Out-In	2.6	Planar + cylindrical 128×32	correlation function, capacity, sumrates, etc.
[24]	Outdoor	2.6	Virtual cylindrical 112×1	sum rates, correlation coefficient, capacity, condition number, etc.
[25]	Indoor	2.4	Planar 64×15	capacity, sum rates, etc.
[26]	Indoor	5.15	Patch+3-D positioner $1 \times (10 \times 10 \times 10)$	inner points, degrees of freedom, etc.
[27]	Indoor	5.3	Two moving TX+ LU Rx/TKK Rx	capacity, sum rates, etc.
[28]	Outdoor	2.6	Virtual ULA 128×1	capacity, sum rates, RMS delay spread, etc.
[29,30]	Outdoor	2.6	Virtual ULA+ cylindrical array 128×128	achieved sum rates, capacity, singular value spreads, etc.
[31]	Indoor	2.70 2.82	24/36-port cube	mutual couplings, capacity, etc.
[32]	Outdoor	2.6	Virtual ULA/ cylindrical array $128 \times 1/128 \times 1$	capacity
[33,34]	Outdoor	3.7	Planar 4×100	Mutual coupling, signal constellation points
[35]	Indoor	2-8	ULA 1×20	channel response, cluster number, angle spread, delay spread, angle PDF, PDP, etc.
[36]	Out-In In-Out-In	2.6	Planar + cylindrical 128×32	RMS delay spread, channel separation, interference power level, etc.
[37]	Reverberation chamber	1	Virtual ULA+ log periodic array(LPA)	average power, K-factor, coherence bandwidth, RMS delay spread, mean delay, spatial correlation, beamforming APS, etc.
[38]	Indoor	5.3	Cylindrical+ semi-spherical 64×21	path loss, PDP, capacity, etc.
[39]	Outdoor	2.6	Virtual ULA 128×1	AoA, delay, complex amplitude, etc.
[40]	Outdoor	28/38/60	ULA 12×4	throughput, reflectivities, etc.

2.1.3 Eigenvalue properties

Eigenvalue distribution of massive MIMO channels was measured in [17], showing that massive MIMO increases channel orthogonality between terminals by increasing the number of transmit antennas. Similar conclusions were drawn in [22,24] via (inverse) condition numbers, in [26] via degrees of freedom, and

in [29] via singular value spreads.

2.1.4 Other channel characteristics

Other channel characteristics such as angle probability density function (PDF), root-mean-square (RMS) delay spread, power delay profile (PDP), angular power spectrum (APS), and correlation between sub-channels were also studied in [22–37]. The authors in [23] considered practical outdoor-to-indoor transmissions and observed that the correlation between subchannels reduces with the increasing number of antennas. As a result, there is hardly any extra gain for more than 20 antennas. Furthermore, cell throughput and reflectivities of massive MIMO with mmWave were measured in [40].

2.2 Challenges for massive MIMO channel measurements

For massive MIMO channels, it is important to measure parameters related to non-stationary properties such as non-stationarities on the array axis as well as on the time axis. However, these parameters are difficult to estimate since they fluctuate from scenarios to scenarios. Hence, a large number of measurement campaigns are required to capture those parameters.

Also, from a realization point of view, the increase of the number of antennas will require many radio frequency (RF) chains and then raise higher requirements for antenna calibrations.

Most of current measurements on massive MIMO channels focus on using uniform linear arrays (ULAs). However, to utilize space compactly, other types of arrays such as planar arrays and cube arrays need to be considered.

2.3 Future directions for massive MIMO channel measurements

Currently, many published measurement results were obtained via virtual antenna arrays. To acquire more realistic channel characteristics, a large physical antenna array is required. In this case, the mutual coupling effect between antenna elements will be considered.

Also, cluster behaviors on the array axis need further investigations. Although cluster appearance and disappearance, and angles of arrival (AoA) shifts were observed in measurements, birth and death rates of clusters and values of AoA shifts are yet to be determined. Moreover, elevation characteristics of massive MIMO channels are less investigated in the literature. The impact of receiver location within the building on measurements is still an open problem to study [41].

Another future direction will be the measurement of massive MIMO in high-speed train (HST), M2M, and mmWave channels. Since HST, M2M, and mmWave communications are key technologies in 5G wireless networks, massive MIMO can be applied to these technologies to boost their performance. In this case, massive MIMO channel characteristics with these technologies will be essential to the system design.

3 Massive MIMO channel models

3.1 Recent advances in massive MIMO channel modeling

Recently, there have been advances in channel models for massive MIMO systems [42]. In general, channel models can be broadly classified into the following categories: correlation-based stochastic models (CBSMs) and geometry-based stochastic models (GBSMs). Additionally, CBSMs can be categorized into two types known as classic i.i.d. Rayleigh fading channel model and correlated channel models. Correlated channel models include the Kronecker-based stochastic model (KBSM), the Weichselberger model [43], and the virtual channel representation (VCR). For KBSM, the spatial correlation matrices at the transmitter and receiver are assumed independent. Conversely, mutual coupling effects between spatial correlation matrices at the transmitter and receiver are modeled in the Weichselberger model and VCR. CBSMs are widely used to evaluate theoretical capacity and performance of massive MIMO systems because they are of lower implementation complexity and mathematically tractable. However,

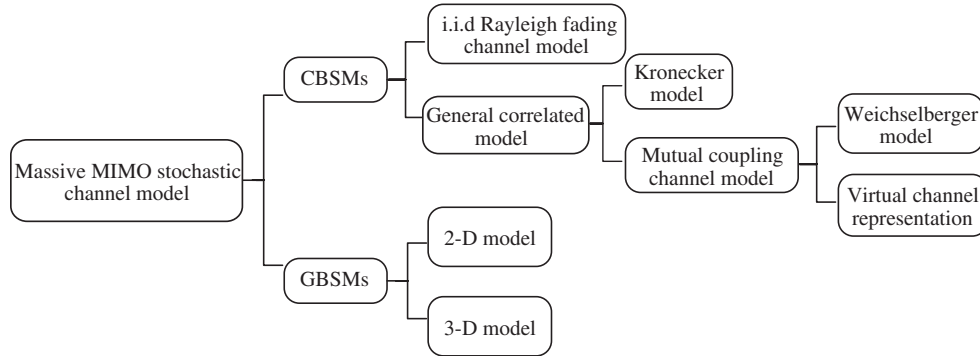


Figure 1 Classification of massive MIMO stochastic channel models.

the accuracy of CBSMs is usually compromised as these models are oversimplified. On the other hand, GBSMs are able to model MIMO channels in a more accurate manner at the cost of higher computational complexity. The classification of massive MIMO stochastic channel models is depicted in Figure 1. In this section, these models [44–57] will be reviewed.

3.1.1 CBSMs

In [44,45], classic i.i.d. Rayleigh fading channel processes were utilized as the channel model for massive MIMO systems. Since the channel coefficients are i.i.d., the central limit theory as well as the random matrix theory can be easily applied to the analysis of massive MIMO channel matrices. However, the i.i.d. Rayleigh channel model ignores the correlation between antennas. Therefore, they are more suitable for widely separated antennas such as massive MIMO systems with distributed antennas than co-located antenna arrays.

Compared with the i.i.d. Rayleigh channel model, KBSM utilized as the channel model for massive MIMO systems in [47,48] considered correlation between antennas. The Kronecker model is of popularity in capacity and performance analysis of massive MIMO systems for its simple implementation and consideration on antenna correlations. However, it forces both link ends to be separable because it neglected the joint correlation between the transmit and receive antenna arrays. Moreover, line-of-sight (LOS) Kronecker models can be found in [49,50].

Reference [46] introduced the Weichselberger channel model which relaxed the separability restriction of the Kronecker model to analyze the performance of massive MIMO systems. This model has the ability to include antenna correlations at both the transmitter and receiver. Furthermore, it jointly considers the correlation between the transmit array and the receive array. The joint correlation was modeled by a coupling matrix, which can be acquired by measurement. Therefore, the Weichselberger channel model achieves a balance between accuracy and complexity for massive MIMO channel models. It can well model co-located antenna scenarios when the coupling effect between the transmit and receive array needs to be taken into account. Also, [46] added the LOS component to the Weichselberger model and henceforth entries of the channel matrix followed Rician fadings. Meanwhile, by eliminating the coupling effect between the transmit and receive antenna arrays, the Weichselberger channel model reduces to the Kronecker model in [46].

The VCR models the MIMO channel by predefined discrete Fourier Transform (DFT) matrices instead of one-sided correlation matrices. As [58] said, its accuracy increases with the number of antennas, as angular bins become smaller. That is to say, the VCR model may play an important role in performance analysis of massive MIMO systems. Channel capacities of VCR were investigated in [51]. However, as pointed out in [59], VCR only supports single polarized ULAs.

Specifically, the Weichselberger model reduces to the virtual channel representation by forcing the eigenbases to be DFT matrices; and it reduces to the Kronecker model by forcing the coupling matrix to be of rank one.

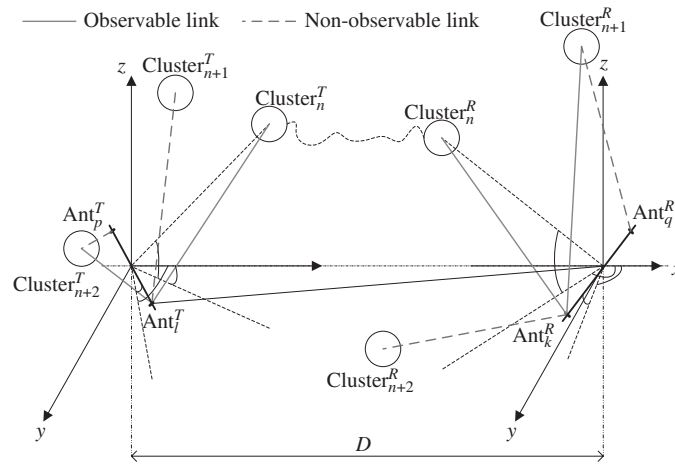


Figure 2 A 3-D wideband twin-cluster massive MIMO channel model in [54].

3.1.2 GBSMs

An extended one-ring channel model [52], a GBSM for narrowband fading channels, has been used to model massive MIMO channel in [53]. It assumed that there were almost no scatters around a highly elevated base station and an infinite number of local scatterers were randomly distributed on a ring around the mobile station. In [53], the APS obeyed the von Mises distribution and the correlation between AoA and angle of departure (AoD) was varying.

A novel non-stationary three-dimensional (3-D) wideband twin-cluster channel model for massive MIMO systems with carrier frequencies on the order of gigahertz (GHz) was proposed in [54]. At the same time, non-stationary properties of clusters such as cluster appearance and disappearance on both the array and time axes were modeled by birth-death processes. The diagram of the channel model in [54] is illustrated in Figure 2. In this figure, examples of non-stationary properties of clusters on the array axis are given. The n th cluster (Cluster $_n$) can be observed by both the l th transmit antenna (Ant $_l^T$) and the k th receive antenna (Ant $_k^R$). However, Cluster $_{n+1}$ is observable to Ant $_k^R$ but not observable to Ant $_l^T$ or Ant $_q^R$, and Cluster $_{n+2}$ is observable to Ant $_l^T$ but not observable to Ant $_p^T$ or Ant $_k^R$. These effects were all modeled under the birth-death process framework in [54]. In addition, spherical wavefront was assumed to model nearfield effects. The impact of the spherical wavefront on the Doppler frequencies on the antenna array is depicted in Figure 3. When the antenna number is growing, the spherical wavefront is more significant. In this case, the larger variation of AoAs results in larger standard deviation of Doppler frequencies. This effect is not captured in conventional MIMO channel models. The non-stationary properties of clusters on the array axis as well as the spherical wavefront effect were also observed in [17]. The impact of elevation angles of clusters on correlation properties was also taken into consideration.

Under a similar birth-death process framework, a wideband two dimensional (2-D) elliptical GBSM for massive MIMO was proposed in [55,56], where clusters were assumed to be located on many confocal ellipses with different major axis lengths to represent different resolvable clusters. In this case, AoD and AoA are dependent, which is different from the model in [54]. Non-stationary properties of clusters in massive MIMO channels were characterized by the birth-death process on both the time and array axes. The APS of AoAs of the massive MIMO channel model in [56] is shown in Figure 4. It can be observed that the AoA is shifting on the array axis due to the spherical wavefront. Also, certain clusters are disappearing and new clusters are appearing. These massive MIMO channel characteristics can all be modeled under the framework in [54–56].

Recently, a GBSM is proposed by the mobile and wireless communications enablers for the METIS project. The METIS GBSM was developed based on the WINNER II channel model, with considerations on spherical wavefronts in order to support massive MIMO channels [57]. The inclusion of spherical wavefront and calculations of AoAs and AoDs are the same as those in [54–56].

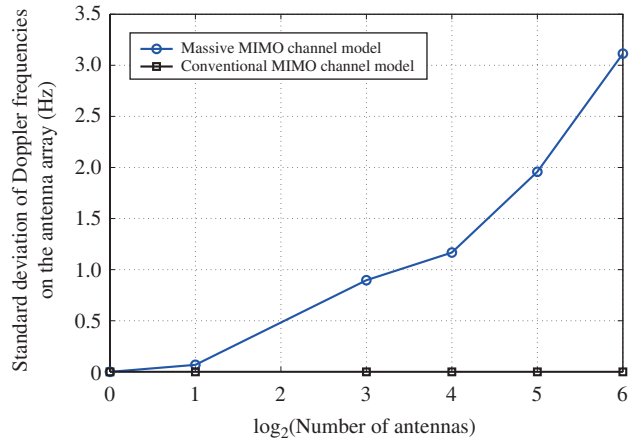


Figure 3 Standard deviations of Doppler frequencies on antenna arrays with different numbers of elements.

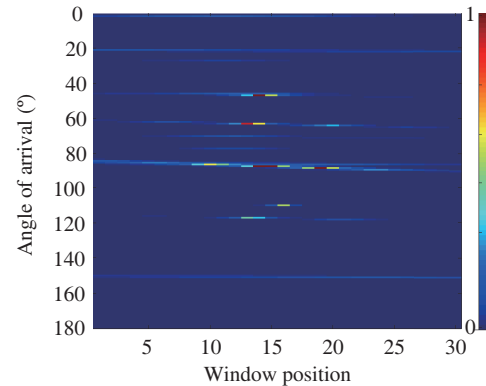


Figure 4 APS of AoAs.

Table 2 Recent advances in massive MIMO channel models

Ref.	Channel model	Complexity	Description
[44,45]	Narrowband i.i.d. Rayleigh	Low	Uncorrelated model
[46–48]	Narrowband CBSM(Kronecker)	Medium	Classic correlated model
[46]	Narrowband CBSM(Weichselberger)	Medium	Jointly correlated model
[51]	Narrowband CBSM(VCR)	Medium	Jointly correlated model
[53]	Extended one-ring GBSM	Medium	Narrowband GBSM
[54]	3-D wideband twin-cluster GBSM	High	Massive MIMO properties considered
[55,56]	2-D wideband ellipse GBSM	High	Massive MIMO properties considered
[57]	3-D wideband GBSM	High	Based on WINNER II channel model

3.1.3 Summary

The above massive MIMO channel models [44–57] are briefly summarized and classified in Table 2. Narrowband CBSMs used in [44–51] are of low complexity, but they are not able to describe the nearfield effect and non-stationary properties, which are two crucial characteristics of massive MIMO channels different from conventional MIMO channels. On the other hand, although the GBSM in [54–56] introduced higher complexity, they properly model important characteristics of massive MIMO channels.

3.2 Challenges for massive MIMO channel modeling

Although there are some advances in massive MIMO channel models, there are still many issues to be resolved [60]. First, the mmWave communication, which is capable of utilizing very large bandwidth (≥ 1 GHz), emerges as a key composite of 5G wireless communication networks [61]. The combination of massive MIMO and mmWave techniques is capable of compensating the large pathloss and atmosphere absorptions of mmWave with large beamforming gain. The design and optimization of future mmWave massive MIMO communication systems is highly influenced by the characteristics of the wireless channel. However, since the time domain resolution is very high (1 ns) in mmWave channels, even the IMT-A channel model which supports up to 5 ns time domain resolution still fails to satisfy the demand of mmWave channels. Consequently, a massive MIMO channel model with improved time resolutions is required in 5G development.

Second, array-time evolution of clusters is modeled by birth-death processes in [54–56]. Applying other stochastic processes to modeling array-time evolution would be challenging. At the same time, replacing stochastic processes with novel methods to model array-time evolution is worth exploring.

Finally, there is a trade-off between channel model accuracy and complexity. In certain situations, a low-complexity and mathematically tractable massive MIMO channel model is preferred when analyzing and simulating system performance. How to find this optimal trade-off remains unanswered.

3.3 Future directions for massive MIMO channel modeling

Solutions are proposed in this section to overcome challenges of massive MIMO modeling. These include the combination of massive MIMO and Saleh-Valenzuela channel model (SV) [62], the combination of massive MIMO and COST 2100 channel model [19–21], massive MIMO channel models for other 5G scenarios, the map-based massive MIMO channel models, and CBSMs for massive MIMO systems. The SV model for massive MIMO channels provides a solution for massive MIMO in mmWave bands. The COST 2100 model for massive MIMO channels is able to naturally model non-stationary properties of clusters on the array axis. Massive MIMO channel models for other 5G scenarios aim at supporting 5G applications such as high-speed train (HST) communications and M2M communications. Ray tracing techniques are applied to the map-based massive MIMO channel models to capture massive MIMO channel characteristics. Finally, CBSMs for massive MIMO systems are of low-complexity and mathematically tractable.

3.3.1 SV model for massive MIMO channels

The SV channel model has been used to evaluate system performance with bandwidth greater than 500 MHz. In this model, rays with different delays within a cluster can be resolved because of the high time resolution, and the number of rays is assumed to follow Poisson distribution [63–67]. The IEEE wireless personal area network (PAN) has applied the SV channel model in its standard [63–67].

To satisfy the mmWave and massive MIMO scenario in 5G communication networks, the current SV channel model should be improved. By applying large antenna arrays, cluster evolution on the array axis modeled by birth-death processes in [54] can be included in the SV model for massive MIMO channels. Meanwhile, updates of geometrical relationships of the channel model are also necessary when non-stationary properties on the time axis are considered. As a result, the cluster generation algorithm in [54] should be improved to support parameter generation for rays within clusters.

Additionally, directional antennas will be widely used in mmWave communication networks to overcome path and atmosphere absorption losses [68]. Consequently, directional antenna characteristics should be incorporated in the SV channel model for massive MIMO. Furthermore, 3-D channels need to be considered to model clusters on the vertical plane [69].

3.3.2 COST 2100 model for massive MIMO channels

The COST 2100 channel model, a cluster-based GBSM, introduced visibility regions (VRs) to model the spatially-variant nature of massive MIMO channels, i.e., cluster appearance and disappearance on the array axis [39]. A VR is a region in space corresponding to a cluster. A cluster is observable to an antenna element if this antenna element lies within the VR of the cluster. Different antenna elements on a large array may lie within various VRs. Then, each antenna element may observe its own set of clusters.

The modeling of spatial variance via VRs in the COST 2100 channel model is fundamentally different from the method based on birth-death processes introduced in the twin-cluster and ellipse channel models in [54–56]. The COST 2100 channel model is able to jointly model time and array evolutions with VRs. Also, it was reported in [39] that parameters of VRs could be estimated based on measured data. For modeling massive MIMO effects at the transmitter and receiver, visibility regions can be applied to both the base station and terminal.

However, the current assumption of a VR is a circular region on the azimuth plane in [19–21,39]. This may fail to model the 3-D scattering environment, especially when the transmitter or receiver moves vertically. A potential solution for this is to generalize circular region of a VR to a sphere in a 3-D space. This extension is depicted in Figure 5. Meanwhile, the complexity of the COST 2100 channel modeling for massive MIMO is still under investigation.

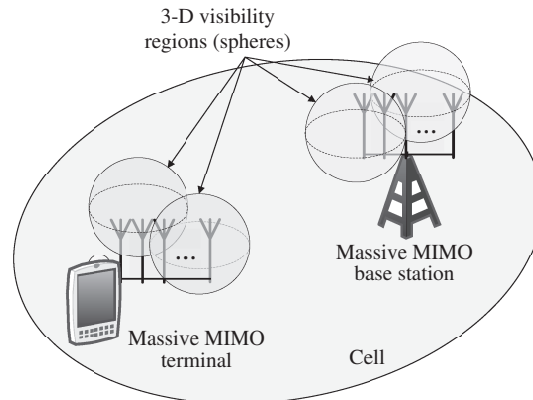


Figure 5 COST 2100 channel model with 3-D visibility regions.

3.3.3 Massive MIMO channel models for other 5G scenarios

It was anticipated in [10–14] that M2M communications would play an essential role in 5G mobile communication systems, where devices were all interconnected. A number of channel models for M2M communications with conventional MIMO can be found in [70–74], where Doppler frequencies were modeled at both the transmitter and receiver. Having the potential to enhance performance, massive MIMO and M2M systems can be combined. Therefore, an M2M massive MIMO channel model should be developed.

The emerging applications of HST communications in 5G mobile communication networks attract researchers to investigate HST channels [75,76]. Massive MIMO equipped at the base station or HST is expected to improve throughput and link reliabilities. However, the high velocities of HST communication systems introduce challenges to channel modeling. One key characteristic is the low stationary interval [76] such that the channel should be modeled as non-stationary [75]. The array-time evolution algorithm proposed in [54–56] can be potentially extended to describe massive MIMO HST channels.

In order to jointly model channel characteristics of other 5G scenarios such as M2M and HST communications, a general massive MIMO channel model which includes Doppler frequencies at both the transmitter and receiver and array-time evolution would be beneficial. These were achieved in a unified GBSM framework developed in [77] by combining the WINNER II and SV models. The unified GBSM framework is shown in Figure 6. In addition, 3-D features and polarization arrays were considered. Furthermore, it was assumed that each ray had its own delay and complex gain in the unified GBSM framework because of the inclusion of the SV model [77].

3.3.4 Map-based massive MIMO channel model

Besides the GBSM discussed in Subsection 3.1.2, the METIS project proposed a novel modeling method for massive MIMO channels named as the map-based channel model (MBCM) [57]. The METIS MBCM was established based on ray tracing techniques. It aimed at tracking each ray from the transmitter to the receiver. Interactions between rays and shadowing/scattering objects such as diffraction, specular reflection, diffuse scattering, and blocking were considered. These shadowing/scattering objects can be randomly generated in the environment or obtained from a specific scenario.

Since each ray is tracked by the MBCM, massive MIMO channel characteristics such as spherical wavefront and non-stationary properties of clusters are included in the model. Additionally, having considered Doppler frequencies at both the transmitter and receiver sides, the METIS MBCM is able to support scenarios where machine-to-machine communications with massive MIMO. However, the ray tracing nature of the MBCM results in high complexity [57]. The practicality of MBCM is to be justified.

3.3.5 Correlation-based massive MIMO channel model

Although GBSMs for massive MIMO channels are able to capture accurate statistical characteristics, they are of high complexity and inconvenient for performance analysis. Therefore, CBSMs with massive

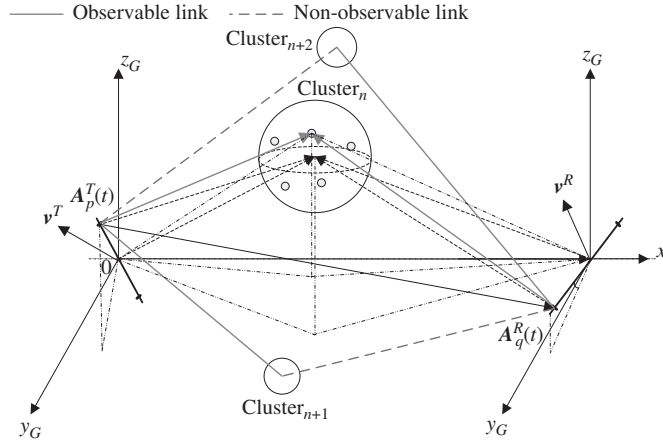


Figure 6 A unified GBSM framework for 5G channels [77].

MIMO channel properties will be another future direction for massive MIMO channel model development because of they are mathematically tractable and of low complexity. In this section, the KBSM-BD-AA for massive MIMO channels in [78] is reviewed.

A conventional KBSM assumes that spatial correlation matrices of the receive arrays and transmit arrays are unrelated. Hence, the channel matrix \mathbf{H} can be expressed as

$$\mathbf{H} = \mathbf{R}_R^{\frac{1}{2}} \mathbf{H}_w \mathbf{R}_T^{\frac{T}{2}}, \quad (1)$$

where \mathbf{H}_w is an $M_R \times M_T$ matrix with zero-mean unit-variance complex i.i.d. Gaussian entries, \mathbf{R}_R and \mathbf{R}_T are overall spatial correlation matrices at the receiver and transmitter, respectively. Additionally, if ULAs are deployed at the receiver and transmitter sides, \mathbf{R}_R and \mathbf{R}_T are Toeplitz matrices [79]. To avoid repeated analysis, we only analyze the receiver side in this paper as the analysis of the transmitter side follows the same procedure. Furthermore, let us denote the complex gain between the k th ($k = 1, 2, \dots$) scatterer and the m th ($m = 1, 2, \dots, M_R$) antenna as s_{mk}^R , the complex gain between the k th scatterer and the n th ($n = 1, 2, \dots, M_R$) antenna as s_{nk}^R . Let $T_{R,mn}$ be the spatial correlation coefficient between the m th and the n th antennas and the entry of matrix \mathbf{T}_R in the m th row and n th column. Then, $T_{R,mn}$ can be computed as

$$T_{R,mn} = \frac{\sum_k s_{mk}^R (s_{nk}^R)^*}{\sqrt{\sum_k |s_{mk}^R|^2} \sqrt{\sum_k |s_{nk}^R|^2}}. \quad (2)$$

In the conventional KBSM, the above discussion implies that all the antennas share the same set of scatterers. In this case, \mathbf{R}_R is equivalent to \mathbf{T}_R , i.e., $\mathbf{T}_R = \mathbf{R}_R$. However, the equivalence between \mathbf{T}_R and \mathbf{R}_R may not hold if antennas do not share the same set of scatterers. In [78], the scatterers in the scatterer set of the m th antenna may not be the same as those of the n th antenna. According to the BD process, the survival probability $E_{R,mn}$ of scatterers when they evolve from the m th antenna to the n th antenna is modeled as

$$E_{R,mn} = e^{-\beta|m-n|}, \quad (3)$$

where $\beta \geq 0$ is a parameter describing how fast a scatterer disappears on the array axis. The antenna correlation coefficient $T'_{R,mn}$ between the m th and n th antennas considering the evolution of scatterer sets on the array axis can be modeled as [78]

$$T'_{R,mn} = E_{R,mn} \frac{\sum_k s_{mk}^R (s_{nk}^R)^*}{\sqrt{\sum_k |s_{mk}^R|^2} \sqrt{\sum_k |s_{nk}^R|^2}} = E_{R,mn} T_{R,mn}. \quad (4)$$

Let $\mathbf{E}_R = [E_{R,mn}]_{M_R \times M_R}$ ($m, n = 1, 2, \dots, M_R$) and $\mathbf{E}_T = [E_{T,pq}]_{M_T \times M_T}$ ($p, q = 1, 2, \dots, M_T$) denote the survival probability matrices at the receiver side and transmitter side. The overall antenna correlation

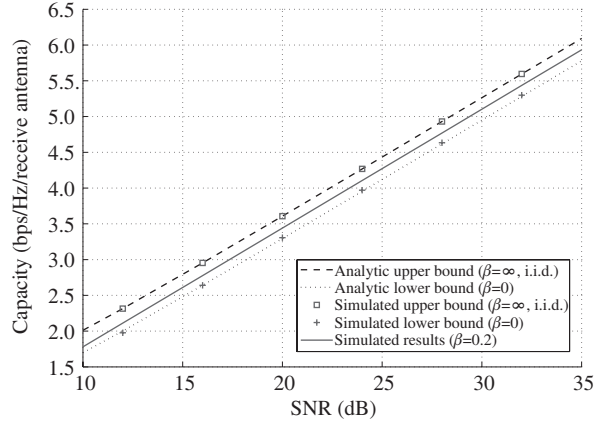


Figure 7 Capacity analysis in the high SNR regime for the KBSM-BD-AA ($M_R = 64, M_T = 32$, half-wavelength ULAs, isotropic scattering environment).

matrices \mathbf{R}_R and \mathbf{R}_T can be represented as $\mathbf{R}_R = \mathbf{T}_R \circ \mathbf{E}_R$ and $\mathbf{R}_T = \mathbf{T}_T \circ \mathbf{E}_T$ where \circ denotes the Hadamard product.

With signal-to-noise ratio (SNR) ρ , combining the receiver and transmitter sides, the capacity lower bound of a massive MIMO system with half-wavelength arrays under isotropic scattering environment in the high SNR regime can be derived as [78]

$$C^L(\rho) \approx C_{\text{iid}}(\rho) + \left(1 + \frac{1}{\gamma}\right) \max \left\{ \log_2 \left(\frac{e}{\pi} \right), \log_2 (1 - e^{-2\beta}) \right\} \quad (5)$$

as $M_R, M_T \rightarrow \infty$, where $C_{\text{iid}}(\rho)$ is the channel capacity of an i.i.d. Rayleigh channel. According to [80], $C_{\text{iid}}(\rho)$ can be computed as

$$C_{\text{iid}}(\rho) = \frac{1}{M_R} \log_2 \det \left(\frac{\rho}{M_T} \mathbf{H}_w \mathbf{H}_w^H \right) = \begin{cases} F(1/\gamma, \gamma\rho), & \gamma \leq 1, \\ \frac{1}{\gamma} F(\gamma, \rho), & \gamma \geq 1, \end{cases} \quad (6)$$

where

$$F(\gamma, \rho) = \log_2 (1 + \rho(\sqrt{\gamma} + 1)^2) + (\gamma + 1) \log_2 \left(\frac{1 + \sqrt{1-a}}{2} \right) - (\log_2 e) \sqrt{\gamma} \frac{1 - \sqrt{1-a}}{1 + \sqrt{1-a}} + (\gamma - 1) \log_2 \left(\frac{1 + \alpha}{\alpha + \sqrt{1-a}} \right) \quad (7)$$

with $a = \frac{4\rho\sqrt{\gamma}}{1 + \rho(\sqrt{\gamma} + 1)^2}$ and $\alpha = \frac{\sqrt{\gamma} - 1}{\sqrt{\gamma} + 1}$.

The channel capacity of KBSM-BD-AA in (5) is depicted in Figure 7 [78]. The simulated results ($\beta = 0.3$) lie within the upper and lower bounds of the channel capacity. The i.i.d. channel model overestimates the channel capacity while the conventional KBSM underestimates the channel capacity of a massive MIMO system.

The adaptation of BD to KBSMs can be achieved without extra complexity, because antenna spatial correlation matrices for KBSMs can be separated easily. However, The adaptation of BD to Weichselber and VCR requires further investigations, which will be an interesting research direction in the future.

Receiver absolute spatial correlation functions and channel capacities of the 2-D ellipse model [56], the 2-D/3-D twin-cluster model [54], the 2-D/3-D unified GBSM framework [77], and the KBSM-BD-AA [78] (isotropic scattering, $\beta = 0.1$) are illustrated in Figures 8 and 9, respectively. As isotropic scattering is assumed in the KBSM-BD-AA, the receiver spatial correlation function of it is significantly different from those of the 2-D ellipse, 2-D/3-D twin-cluster, and the 2-D/3-D unified GBSM framework. The channel capacities of the 3-D twin-cluster model and the unified GBSM framework are similar as the twin-cluster model is a special case of the unified GBSM framework. On the other hand, KBSM-BD-AA has lower antenna correlations as shown in Figure 8. Consequently, the channel capacity of the KBSM-BD-AA is higher than that of other models.

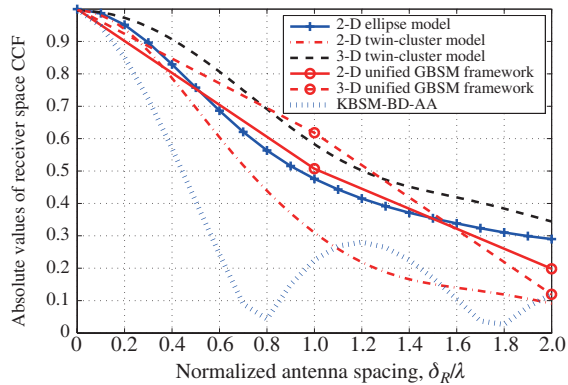


Figure 8 Receiver absolute spatial correlation functions of the 2-D ellipse model [56], the 2-D/3-D twin-cluster model [54], the 2-D/3-D unified GBSM framework [77], and the KBSM-BD-AA [78].

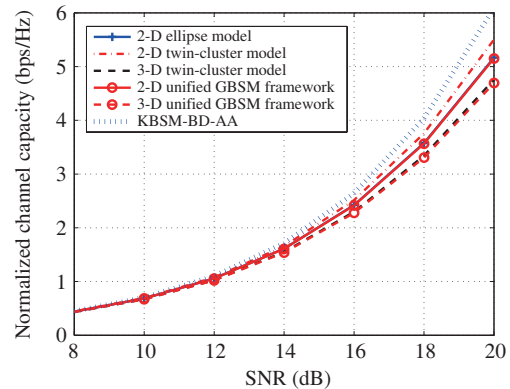


Figure 9 Channel capacities of the 2-D ellipse model [56], the 2-D/3-D twin-cluster model [54], the 2-D/3-D unified GBSM framework [77], and the KBSM-BD-AA [78].

4 Conclusion

In this paper, recent advances, challenges, and future directions of channel measurements and channel models for massive MIMO communication systems have been analyzed. Measurements have revealed that certain benefits and effects of channel models for conventional MIMO systems are not valid for massive MIMO channels. Massive MIMO channel characteristics such as the spherical wavefront effect and non-stationary properties on the antenna array have significant impacts on channel models. Therefore, they should be taken into account in massive MIMO channel model developments. Recent CBSMs and GBSMs for massive MIMO channels have been compared, showing that GBSMs are more natural to capture the characteristics of massive MIMO channels, although they have higher computational complexity. Then, a number of future massive MIMO channel models based on the SV channel model, the COST 2100 channel model, the METIS MBCM, massive MIMO channel models for other 5G scenarios, and CBSMs have been discussed. These models aim to capture key characteristics of various scenarios emerging in 5G communication networks and provide different trade-off between model accuracy and complexity.

Acknowledgements

This work was supported by EU FP7 QUICK Project (Grant No. PIRSES-GA-2013-612652), EU H2020 ITN 5G Wireless Project (Grant No. 641985), National Natural Science Foundation of China (Grant No. 61210002), MOST 863 Project in 5G (Grant No. 2014AA01A706), and International S&T Cooperation Program of China (Grant No. 2014DFA11640).

Conflict of interest The authors declare that they have no conflict of interest.

References

- 1 Nokia Networks. Looking ahead to 5G. White Paper. http://info.networks.nokia.com/LookingAheadto5G_5G_Requirements_wp.html
- 2 Samsung. 5G vision. White Paper. <http://www.samsung.com/global/business-images/insights/2015/Samsung-5G-Vision-2.pdf>
- 3 Dahlman E, Mildh G, Parkvall S, et al. 5G radio access. Ericsson Rev, 2014, 6: 1–7. http://sixtysix.wirelab.ericsson.net/res/thecompany/docs/publications/ericsson_review/2014/er-5g-radio-access.pdf
- 4 Qualcomm. 1000x data challenge. White Paper. <https://www.qualcomm.com/documents/1000x-mobile-data-challenge>
- 5 Huawei. 5G a technology vision. White Paper. https://www.huawei.com/ilink/en/download/HW_314849
- 6 CMCC. CMCC technology vision 2020 plus. White Paper. http://www.gtigroup.org/CMCC_Technology_Vision_2020_Plus.White_Paper.pdf

- 7 METIS. Scenarios, requirements and KPIs for 5G mobile and wireless system. http://publications.lib.chalmers.se/records/fulltext/213055/local_213055.pdf
- 8 IMT-2020 Promotion Group. 5G visions and requirements. White Paper. <http://www.imt-2020.cn/en/documents/listByQuery?currentPage=1&content=>
- 9 5GNOW. 5G cellular communications scenarios and system requirements. <http://is-wireless.com/wp-content/uploads/2015/07/5GNOW-Deliverables-5G-Cellular-Communications-Scenarios-and-System-Requirements.pdf>
- 10 Wang C X, Haider F, Gao X, et al. Cellular architecture and key technologies for 5G wireless communication networks. *IEEE Commun Mag*, 2014, 52: 122–130
- 11 Tse D, Viswanath P. *Fundamentals of Wireless Communication*. Cambridge: Cambridge University Press, 2005
- 12 Larsson E G, Tufvesson F, Edfors O, et al. Massive MIMO for next generation wireless systems. *IEEE Commun Mag*, 2014, 52: 186–195
- 13 Rusek F, Persson D, Lau B K, et al. Scaling up MIMO: opportunities and challenges with very large arrays. *IEEE Signal Processing Mag*, 2012, 30: 40–60
- 14 Ma Z, Zhang Z Q, Ding Z G, et al. Key techniques for 5G wireless communications: network architecture, physical layer, and MAC layer perspectives. *Sci China Inf Sci*, 2015, 58: 041301
- 15 Jungnickel V, Manolakis K, Zirwas W, et al. The role of small cells, coordinated multipoint, and massive MIMO in 5G. *IEEE Commun Mag*, 2014, 52: 44–51
- 16 Osseiran A, Boccardi F, Braun V, et al. Scenarios for 5G mobile and wireless communications: the vision of the METIS project. *IEEE Commun Mag*, 2014, 52: 26–35
- 17 Payami S, Tufvesson F. Channel measurements and analysis for very large array systems at 2.6 GHz. In: *Proceedings of 6th European Conference on Antennas and Propagation (EUCAP)*, 2012, Prague. 1–8
- 18 Kyösti P, Meinilä J, Hentilä L, et al. WINNER D1.1.2 WINNER II channel models. ver 1.1, 2007
- 19 Liu L, Oestges C, Poutanen J, et al. The COST 2100 MIMO channel model. *IEEE Commun Mag*, 2012, 19: 92–99
- 20 Zhu M F, Eriksson G, Tufvesson F. The COST 2100 channel model: parameterization and validation based on outdoor MIMO measurements at 300 MHz. *IEEE Trans Wirel Commun*, 2013, 12: 888–897
- 21 Verdone R, Zanella A. *Pervasive Mobile and Ambient Wireless Communications: COST Action 2100*. London: Springer, 2012
- 22 Li J, Zhao Y. Channel characterization and modeling for large-scale antenna systems. In: *Proceedings of 14th International Symposium on Communications and Information Technologies (ISCIT)*, Incheio, 2014. 559–563
- 23 Gao X, Edfors O, Rusek F, et al. Linear pre-coding performance in measured very-large MIMO channels. In: *Proceedings of IEEE Vehicular Technology Conference (VTC Fall)*, San Francisco, 2011. 1–5
- 24 Hoydis J, Hoek C, Wild T, et al. Channel measurements for large antenna arrays. In: *Proceedings of International Symposium on Wireless Communication Systems (ISWCS)*, Paris, 2012. 811–815
- 25 Shepard C, Yu H, Anand N, et al. Argos: practical many-antenna base stations. In: *Proceedings of 18th Annual International Conference on Mobile Computing and Networking*, Istanbul, 2012. 53–64
- 26 Bernland A, Gustafsson M. Estimation of spherical wave coefficients from 3-D positioner channel measurements. *IEEE Antenn Wirel Propag Lett*, 2012, 11: 608–611
- 27 Rusek F, Edfors O, Tufvesson F. Indoor multi-user MIMO: measured user orthogonality and its impact on the choice of coding. In: *Proceedings of 6th European Conference on Antennas and Propagation (EUCAP)*, Prague, 2012. 2289–2293
- 28 Payami S, Tufvesson F. Delay spread properties in a measured massive MIMO system at 2.6 GHz. In: *Proceedings of IEEE 24th International Symposium on Personal Indoor and Mobile Radio Communications (PIMRC)*, London, 2013. 53–57
- 29 Gao X, Edfors O, Rusek F, et al. Massive MIMO in real propagation environments. *IEEE Trans Wirel Commun*, in press
- 30 Gao X, Tufvesson F, Edfors O, et al. Measured propagation characteristics for very-large MIMO at 2.6 GHz. In: *Conference Record of 46th Asilomar Conference on Signals, Systems and Computers (ASILOMAR)*, Pacific Grove, 2012. 295–299
- 31 Chiu C Y, Yan J B, Murch R D. 24-port and 36-port antenna cubes suitable for MIMO wireless communications. *IEEE Trans Antenn Propag*, 2008, 56: 1170–1176
- 32 Gao X, Edfors O, Liu J, et al. Antenna selection in measured massive MIMO channels using convex optimization. In: *Proceedings of IEEE Global Communications Conference*, Atlanta, 2013. 129–134
- 33 Vieira J, Rusek F, Tufvesson F. Reciprocity calibration methods for massive MIMO based on antenna coupling. In: *Proceedings of IEEE Global Communications Conference*, Austin, 2014. 3708–3712
- 34 Vieira J, Malkowsky S, Nieman K, et al. A flexible 100-antenna testbed for massive MIMO. In: *Proceedings of IEEE Global Communications Conference*, Austin, 2014. 1–7
- 35 Poon S Y, Ho M. Indoor multiple-antenna channel characterization from 2 to 8 GHz. In: *Proceedings of IEEE International Conference on Communications*, Anchorage, 2003. 3519–3523
- 36 Gao X, Glazunov A A, Weng J, et al. Channel measurement and characterization of interference between residential femto-cell systems. In: *Proceedings of 5th European Conference on Antennas and Propagation (EUCAP)*, Rome, 2011. 3769–3773

- 37 Glazunov A A, Prasad S, Handel P. Experimental characterization of the propagation channel along a very large virtual array in a reverberation chamber. *Prog Electromagn Res B*, 2014, 59: 205–217
- 38 Koivunen J, Almers P, Kolmonen V M, et al. Dynamic multi-link indoor MIMO measurements at 5.3 GHz. In: *Proceedings of 2nd European Conference on Antennas and Propagation*, Edinburgh, 2007. 1–6
- 39 Gao X, Tufvesson F, Edfors O. Massive MIMO channels-measurements and models. In: *Proceedings of Asilomar Conference on Signals, Systems and Computers*, Pacific Grove, 2013. 280–284
- 40 Pi Z Y, Khan F. A millimeter-wave massive MIMO system for next generation mobile broadband. In: *Proceedings of Asilomar Conference on Signals, Systems and Computers*, Pacific Grove, 2012. 693–698
- 41 Molisch A F, Tufvesson F. Propagation channel models for next-generation wireless communications systems. *IEICE Trans Commun*, 2014, E97-B: 2022–2034
- 42 Zheng K, Ou S L, Yin X F. Massive MIMO channel models: a survey. *Hindawi International J Antenn Propag*, 2014: 1–10
- 43 Weichselberger W, Herdin H, Özcelik H, et al. A stochastic MIMO channel model with joint correlation of both link ends. *IEEE Trans Commun*, 2006, 5: 90–100
- 44 Mohammed S K, Larsson E G. Per-antenna constant envelope precoding for large multi-user MIMO systems. *IEEE Trans Commun*, 2013, 61: 1059–1071
- 45 Zhang J W, Yuan X J, Ping L. Hermitian precoding for distributed MIMO systems with individual channel state information. *IEEE J Sel Areas Commun*, 2013, 31: 241–250
- 46 Wen C K, Jin S, Wong K K. On the sum-rate of multiuser MIMO uplink channels with jointly-correlated Rician fading. *IEEE Trans Commun*, 2011, 59: 2883–2895
- 47 Noh S, Zoltowski M D, Love D J. Pilot beam pattern design for channel estimation in massive MIMO systems. *IEEE J Sel Top Signal Process*, 2014, 8: 787–801
- 48 Couillet R, Debbah M, Silverstein J W. A deterministic equivalent for the analysis of correlated MIMO multiple access channels. *IEEE Trans Inf Theory*, 2011, 57: 3493–3514
- 49 Taricco G. Asymptotic mutual information statistics of separately correlated Rician fading MIMO channels. *IEEE Inf Theory*, 2008, 54: 3490–3504
- 50 Riegler E, Taricco G. Asymptotic statistics of the mutual information for spatially correlated Rician fading MIMO channels with interference. *IEEE Inf Theory*, 2010, 56: 1542–1559
- 51 Veeravalli V V, Liang Y, Sayeed A M. Correlated MIMO wireless channels: capacity, optimal signaling, and asymptotics. *IEEE Inf Theory*, 2005, 51: 2058–2072
- 52 Zhang M, Smith P J, Shafi M. An extended one-ring MIMO channel model. *IEEE Trans Wirel Commun*, 2007, 6: 2759–2764
- 53 Chen J, Lau V K N. Two-Tier precoding for FDD multi-Cell massive MIMO time-varying interference networks. *IEEE J Sel Areas Commun*, 2014, 32: 1230–1238
- 54 Wu S, Wang C X, Aggoune E -H M, et al. A non-stationary 3-D wideband twin-cluster model for 5G massive MIMO channels. *IEEE J Sel Areas Commun*, 2014, 32: 1207–1218
- 55 Wu S B, Wang C X, Aggoune E -H M. Non-stationary wideband channel models for massive MIMO systems. In: *Proceedings of 2nd Symposium on Wireless Sensor and Cellular Networks*, Jeddah, 2013. 1–8
- 56 Wu S B, Wang C X, Haas H, et al. A non-stationary wideband channel model for Massive MIMO communication systems. *IEEE Trans Wirel Commun*, 2015, 14: 1434–1446
- 57 Raschkowski L, Kyosti P, Kusume K, et al. METIS channel models. https://www.metis2020.com/wp-content/uploads/deliverables/METIS_D1.4.v1.0.pdf
- 58 Ozcelik H, Czinik N, Bonek E. What Makes a Good MIMO Channel Model? In: *Proceedings of IEEE 61st Vehicular Technology Conference*, Stockholm, 2005. 156–160
- 59 Sayeed A M. Deconstructing multiantenna fading channels. *IEEE Trans Signal Process*, 2002, 50: 2563–2579
- 60 Medbo J, Borner K, Haneda K, et al. Channel modelling for the fifth generation mobile communications. In: *Proceedings of 8th European Conference on Antennas and Propagation (EuCAP)*, Hague, 2014. 219–223
- 61 Andrews J G, Buzzi S, Choi W, et al. What will 5G be? *IEEE J Sel Areas Commun*, 2014, 32: 1065–1082
- 62 Saleh A A M, Valenzuela R A. A statistical model for indoor multipath propagation. *IEEE J Sel Areas Commun*, 1987, 5: 128–137
- 63 Molisch A F, Balakrishnan K, Cassioli D, et al. IEEE 802.15.4a channel model—final report. <https://mentor.ieee.org/802.15/dcn/04/15-04-0662-04-004a-channel-model-final-report-r1.pdf>
- 64 Porcino D, Hirt W. Ultra-wideband radio technology: potential and challenges ahead. *IEEE Commun Mag*, 2003, 41: 66–74
- 65 Fort A, Ryckaert J, Desset C, et al. Ultra-wideband channel model for communication around the human body. *IEEE J Sel Areas Commun*, 2006, 24: 927–933
- 66 Molisch A F, Foerster J R, Pendergrass M. Channel models for ultrawideband personal area networks. *IEEE Wirel Commun*, 2004, 10: 14–21
- 67 Maltsev A, Sadri A, Maslennikov R, et al. Channel models for 60 GHz WLAN systems. Doc.: IEEE 802.11-09/0334r6, 2010

- 68 Rappaport T S, Sun S, Mayzus R, et al. Millimeter wave mobile communications for 5G cellular: it will work! *IEEE Access*, 2013, 1: 335–349
- 69 3GPP TR 36.873. Study on 3D channel model for LTE. V2.0.0, 2014
- 70 Cheng X, Yao Q, Wen M W, et al. Wideband channel modeling and ICI cancellation for vehicle-to-vehicle communication systems. *IEEE J Sel Areas Commun*, 2013, 31: 434–448
- 71 Cheng X, Wang C X, Ai B, et al. Envelope level crossing rate and average fade duration of non-isotropic vehicle-to-vehicle Ricean fading channels. *IEEE Trans Intell Transp Syst*, 2013, 15: 62–72
- 72 Karedal J, Tufvesson F, Czink N, et al. A geometry-based stochastic MIMO model for vehicle-to-vehicle communications. *IEEE Trans Wirel Commun*, 2009, 8: 3646–3657
- 73 Zajić A G, Stüber G L. Three-dimensional modeling and simulation of wideband MIMO mobile-to-mobile channels. *IEEE Trans Wirel Commun*, 2009, 8: 1260–1275
- 74 Yuan Y, Wang C X, Cheng X, et al. Novel 3D geometry-based stochastic models for non-isotropic MIMO vehicle-to-vehicle channels. *IEEE Trans Wirel Commun*, 2014, 13: 298–309
- 75 Ghazal A, Wang C X, Ai B, et al. A nonstationary wideband MIMO channel model for high-mobility intelligent transportation systems. *IEEE Trans Intell Transp Syst*, 2015, 16: 885–897
- 76 Chen C, Zhong Z, Ai B. Stationarity intervals of time-variant channel in high speed railway scenario. *China Commun*, 2012, 9: 64–70
- 77 Wu S B, Wang C X, Aggoune E -H M, et al. A novel Kronecker-based stochastic model for massive MIMO channels. In: *Proceedings of IEEE/CIC International Conference on Communications in China, Shenzhen, 2015*
- 78 Chuah C N, Tse D N C, Kahn J M, et al. Capacity scaling in MIMO wireless systems under correlated fading. *IEEE Trans Inf Theory*, 2002, 48: 637–650
- 79 Wu S B, Wang C X, Aggoune E -H M, et al. A unified framework for 5G wireless channel models. *IEEE Trans Wirel Commun*, submitted for publication
- 80 Tulino A M, Verdú S. Random matrix theory and wireless communications. *Found Trends Commun Inf Theory*, 2004, 1: 1–182